Materials Chemistry and Physics 212 (2018) 274–281

Contents lists available at ScienceDirect

Materials Chemistry and Physics

journal homepage: www.elsevier.com/locate/matchemphys

Polystyrene photonic crystals as optical sensors for volatile organic compounds

L. Burratti [a], F. De Matteis [a, b, c], M. Casalboni [a, b, c], R. Francini [a, c], R. Pizzoferrato [a], P. Prosposito [a, b, c, *]

[a] Industrial Engineering Department, University of Rome Tor Vergata, 00133 Rome, Italy
[b] National Interuniversity Consortium of Materials Science and Technology, INSTM, University of Rome Tor Vergata, 00133 Rome, Italy
[c] Center for Regenerative Medicine - CIMER, University of Rome Tor Vergata, 00133 Rome, Italy

HIGHLIGHTS

- Self-assembled polystyrene photonic crystals.
- Bragg diffraction of nanospheres photonic crystals.
- Optical sensor of organic vapour compounds based on change of the reflective spectra.
- Breathalyzer to detect the presence of ethanol in drivers' breath.

ARTICLE INFO

Article history:
Received 31 July 2017
Received in revised form
13 March 2018
Accepted 15 March 2018
Available online 20 March 2018

Keywords:
Photonic crystals
Polystyrene nanoparticles
Volatile organic compounds
Alcohol's sensors
Optical sensors

ABSTRACT

We have synthesized self-assembled photonic crystals (PCs) based on polystyrene nanospheres having average diameters of 250 nm. Samples were obtained by drop-casting technique and subsequent self-assembly on pre-treated glass substrates to increase the surface wettability. Films showed a very good reflectance band with a maximum at 600 nm. We studied the reflectance peak changes as a function of time in presence of vapours of different alcohols. Specifically, we investigated methanol, ethanol, 1-propanol, isopropanol and n-butanol in order to test the potentiality of the system as optical gas sensor for volatile organic compounds (VOCs). We found a considerable redshift of the reflectance band in the presence of the alcohols that cannot be explained only on the basis of the different refractive index of the solvents. We attributed this behaviour to a cooperative effect due to an increase of the effective refractive index and to a swelling process of the polystyrene nanospheres induced by the contact with the alcohols. A different behaviour was found for water due to the hydrophobic properties of the surface of the polymeric photonic crystals. This property was exploited to test the polystyrene PCs for the measurement of the relative concentration of ethanol vapour in a closed volume exploiting different ethanol/water concentrations for a possible use as breathalyzer. The estimated limit of detection (LOD) of ethanol vapour for our system was 2% (v_{Ethan}/v_{tot}) corresponding to 1167 ppm.

1. Introduction

Environmental pollution such as the poisoning of drinking water and the air contamination is a huge problem for human and planet health [1,2]. Between the most common contaminants an important role is represented by heavy metals [3–6], inorganic gases and volatile organic compounds (VOCs) [7], which come from industrial processes or from the use of pesticides and fertilizers in agriculture. These chemical toxic compounds, once released into the environment (in water, air or soil) do not remain confined to restricted areas, but easily expand into larger areas. Thus, every day we are exposed to pollutants through the air, water and the food [8,9], causing serious allergies and pathologies like asthma or in some cases worse diseases such as cancer.

As mentioned, VOCs are a class of toxic compounds, which have high vapour pressure at room temperature and are very common as contaminants [10]. If a proper ventilation of indoor spaces is not

* Corresponding author. Industrial Engineering Department, University of Rome Tor Vergata - 00133 Rome, Italy.
E-mail address: paolo.prosposito@uniroma2.it (P. Prosposito).

https://doi.org/10.1016/j.matchemphys.2018.03.039
0254-0584/

provided, the volatile compounds stagnate and people can be exposed to high VOCs concentration for long times, with dangerous risks for health. In fact, data from various samples in the United States show that within residential and workplace environments, people are exposed to many different kinds of VOCs [11]. Alcohols are a class of VOCs, of which the most common are methanol, ethanol, 1-propanol, isopropanol and n-butanol. Each of these alcohols causes different deleterious effects on the human body by contact, ingestion or inhalation. For instance, 100 ml of pure methanol can lead to death if ingested [12], isopropanol causes serious eye irritation and it may lead to drowsiness or dizziness [13], n-butanol is harmful if swallowed and it causes skin irritation and serious eye damage [14]. Additionally, vapours and liquids of these alcohols are highly flammable with obvious risks on work safety. For all these reasons it is extremely important to be able to detect the presence of even small amounts of these contaminants and to this end, it is essential the development of devices with the ability to detect their presence. Usually, devices to detect VOCs are solid-state multisensor systems, often referred to as *electronic nose* [15]. These electronic devices can be made up by conducting polymers [16,17] or semiconducting metal oxides [18–22], which are both based on a conductivity change after the exposure to the gas. These types of solid-state sensors are difficult to produce and expensive, hence, the development of innovative and low cost sensors based on different detection mechanisms is highly demanded.

Optical sensors [23–27], in which the presence of contaminants results in a change of optical properties (phosphorescence, fluorescence, Raman scattering, reflectance, and transmittance) are an attractive alternative both for the absence of electrical signals, which can be dangerous in specific environments, and for their potential high sensitivity. Recently, gas sensors based on Photonic Crystals (PCs) have been studied since they are easy to realize and less expensive than others solid-state sensors [28–32]. PCs are devices formed by microstructured dielectric materials with periodic spatial modulation of the dielectric function (DF) that produces photonic band gaps or stop gaps [33]. When a visible light beam hits a PC, some frequencies cannot propagate inside the band gap, since the light, interacting with the microstructures, has a destructive interference and the relative frequencies are reflected [34–36]. Consequently, the density of allowed photonic states can be strongly affected in the spectral region of the stop band and peculiar photonic properties has been reported leading to photonic crystal lasing [37,38]. The photonic band gap can be determined by optical measurement such as reflectance, where the maximum of the reflected wavelength is related to PC microstructure and the specific refractive index (RI) of the material [39]. The working principle of the PC based sensors is a change of the reflectance peak energy and shape induced by a change of the RI of system [27–33,40–42].

Very recently, these types of sensors found also another important application as breathalyzers [28,29,43]. The breathalyzers are devices able to detect the presence of ethanol in drivers' breath. This perspective is very fascinating since the World Health Organization valued that more than one million people die annually in road crashes and the majority of these are due to driving under the influence of alcohol and drugs [44,45]. To prevent road accidents, it is important to be able to determine a drunk driver quickly, accurately and in a non-invasive way. The two most widely used types of breathalyzers are: the disposable ones, which are very cheap but have the disadvantages to be strongly sensible to change of temperature and humidity, and the more expensive and sophisticated ones, which need a constant recalibration [46]. Even in this case, optical devices based on PCs can be of help in this field for their low cost, easy of fabrication and adequate sensibility if appropriately developed.

In this paper, we have synthesized good quality PCs based on opal films with commercial polystyrene (PS) nanoparticles by drop-casting on pre-treated glass substrates. The opal films presented a very good reflectivity band with a maximum around 600 nm. We studied time-dependence of reflectance peak of photonic crystals in the presence of different alcohol vapours. We tested PCs samples as alcohols gas detectors with methanol, ethanol, 1-propanol, isopropanol and n-butanol as analytes. Moreover, we used PS PCs to measure the relative concentration of ethanol in a closed volume exploiting different ethanol/water concentrations (v_{Ethan}/v_{tot}). The estimated LOD of our system is 2% of ethanol.

2. Experimental

2.1. Materials

Polystyrene nanospheres (mean nominal diameter D = 250 nm) were purchased from *Microparticles GmbH*. The beads are dispersed as colloids in water solution with concentration of 2.5% wt. The investigated VOCs were produced by evaporation of high purity solvents, specifically methanol, ethanol, 1-propanol, isopropanol and n-butanol that were purchased from *Sigma-Aldrich* and used without further purification. The substrates for the sample deposition were commercial Corning® glass slides ($2.5 \times 2.5\ cm^2$). Substrates were previously treated with the following procedure. They were immersed in a solution H_2SO_4/H_2O_2 (3:1, volume ratio) for 10 min, then in a solution of $NH_4OH/H_2O_2/H_2O$ (1:0.6:0.8, volume ratios) for 5 min in ultrasonic bath, and finally in $HCl/H_2O_2/H_2O$ (1:2:7, volume ratios) for 5 min. As a final step, the substrates were washed with deionized water and dried by N_2 gas. All the chemicals for the substrate treatment namely sulfuric acid (98%), hydrogen peroxide (35%, in water solution), ammonium hydroxide (40%) and hydrochloric acid (37%) were purchased from *Sigma Aldrich*.

2.2. Photonic crystals synthesis

A microscope BK7 glass slide was used as substrate; a circular polymeric mask was placed onto the glass to spatially limit the spreading of the colloidal solution on the surface, to increase the structural order of the photonic crystals and to enhance the intensity of reflected light. The PCs fabrication starts from colloidal solution. A volume of 230 μl was spread onto the treated glass, inside the useful circular area. After deposition, samples were dried at 25 °C for 24 h in an incubator having a controlled humidity. This procedure was necessary to have good PCs with a suitable reflectance and a high mechanical stability.

2.3. Apparatus

The reflectance spectra were recorded by an ellipsometer Wvase 32 (*J.A. Woollam*) at different angles from 30° to 70°. In order to perform reflectance measurements at normal incidence and with a specific gas environment we fabricated a suitable sample chamber. Fig. 1 reports a schematic drawn of the experimental set-up used for reflectance measurements at normal incidence. In the supporting information, in figure SI_1, is reported a photograph of the real experimental set-up. The sample is mounted on the basis of the measurement chamber and is coupled with a halogen lamp (DH-2000, *OceanOptics*) through an optical fiber. The fiber enables the optical excitation by means of a specific lens producing a parallel light beam. The reflected light from the PC is collected back by the same lens and sent through a second optical fiber to a compact spectrophotometer (*Flame*, *OceanOptics*) which allows the recording and analysis of the reflected beam. SEM images were

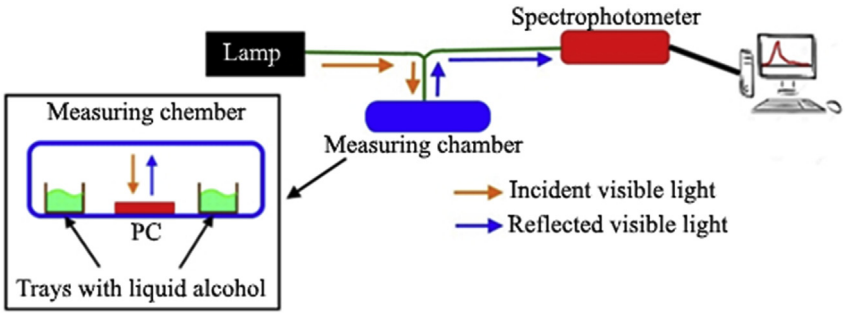

Fig. 1. Experimental set-up for reflectance measurements at normal incidence.

obtained with *SUPRA 35 LEO* field emission scanning electron microscope. Dynamic Light Scattering (DLS) measurements were recorded by a Malvern Zetasizer Nanoseries instrument (Malvern, UK) equipped with a 10 mW HeNe laser at 632.8 nm wavelength.

2.4. Detection of VOCs by photonic crystals

To investigate the change of the optical properties of the PC as a function of the environmental conditions we inserted into the measuring chamber three little jars able to be filled with the specific solvents. The small containers were filled with a total volume of 600 μl of the selected alcohol, then we closed the chamber and we started the measurement collecting the reflectance spectra as a function of time. We recorded reflected spectrum every 30 s for 2 h. The analysis was also performed for pure water, to test the response of the optical sensor in presence of high percentage of humidity and to understand if water can produce a variation of the reflected signal independently from the specific investigated solvents. In order to detect ethanol vapours of different concentrations, we prepared ethanol/water solutions changing the relative volumes of the two components. The experimental procedure was the same as the one used for pure alcohols.

3. Results and discussions

The photonic crystals diffraction behaviour can be described by a combination of Bragg and Snell's laws [41,47–49] that for an *fcc* structure gives:

$$m\lambda_{max} = 2\sqrt{\frac{2}{3}}D\sqrt{n_{eff.}^2 - sin^2\theta} \quad (1)$$

where m is the diffraction order, λ_{max} is the wavelength of the maximum of the diffraction peak, D is the diameter of the nanospheres, θ is the incident angle of light and n_{eff} is the effective refractive index. For opal structure, the effective refractive index is [28,48]:

$$n_{eff.} = \sqrt{fn_p^2 + (1-f)n_m^2} \quad (2)$$

where n_p and n_m are the refractive indexes of the particles and of the material between the dielectric spheres (generally air), respectively, f is the volume fraction (known as filling factor) of the particles in *fcc* structure (for an ideal lattice is 0.74). In general, this kind of optical sensors are based on the effects of a change of n_{eff}. If the dielectric material into voids between particles is changed, n_m and the total effective RI change consequently. If all the other parameters are the same (specifically the angle of incidence and the diameter of the spheres), the final effect is a shift of the diffracted wavelength maximum.

3.1. Optical and structural characterization of photonic crystals

We determined the f value of polystyrene PCs by reflection spectra at various angles. In figure SI_2 are reported, as an example, reflectance spectra of the PC at three different angles of incidence obtained with the ellipsometer set-up. Fig. 2 displays the wavelength of the measured reflectance peaks (red circles) vs incident angle while the continuous blue line shows the fitting with the Bragg-Snell's law (eq. (1)). The PCs behaviour is in good agreement with theoretical previsions. The values of filling factor and particles diameter can be derived from fitting parameters. By the analysis, we obtained 0.72 ± 0.04 and 245 ± 5 nm for the filling factor and diameter, respectively. Fig. 3 shows SEM micrographs of the PC. Fig. 3(a) is a SEM image of the PC taken perpendicularly to the external surface, while Fig. 3(b) is a cross sectional SEM image showing the layers composing the photonic crystal. The sample is a multilayer composed by around 25 layers. A not perfect packing of the nanobeads can be easily observed, this arrangement could explain the value of the filling factor f, which slightly deviates from the ideal case. By the SEM micrograph analysis of all the particles present in the picture, we obtained a mean diameter of 244 ± 7 nm. Analysing the SEM image we estimated also the polydispersity index (PDI) of the nanobeads following the indications given in literature for polymeric spheres [50,51]. We estimated a PDI of 1.002 which indicates a very good monodispersion of our system.

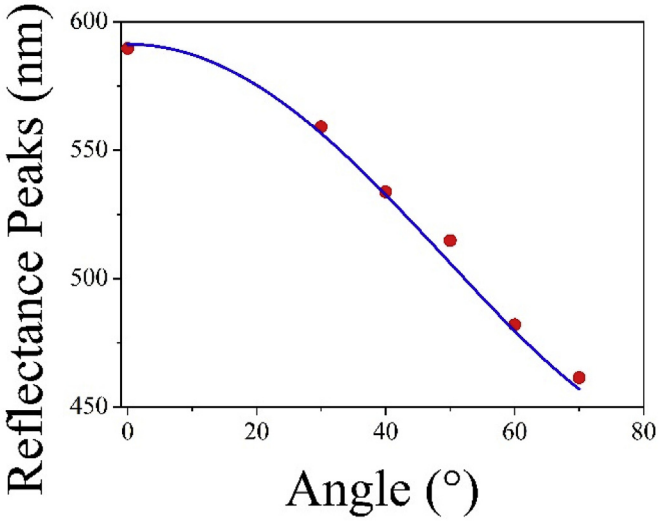

Fig. 2. Reflectance peaks as a function of incident light angles (red circles). The solid line (blue) represents the fitting curve obtained with Bragg-Snell's law. (For interpretation of the references to colour in this figure legend, the reader is referred to the Web version of this article.)

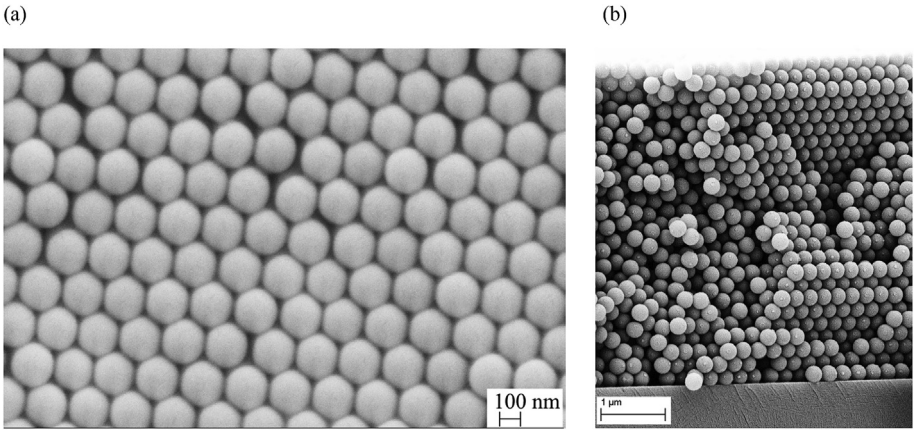

Fig. 3. SEM micrograph of polystyrene PC sample: (a) portion of external surface; (b) cross section.

These results are in excellent agreement with the results obtained by the fitting analysis and the DLS characterization presented in the next chapter.

3.2. Response of the polystyrene photonic crystal to alcohols

The optical response of the PC to different solvents has been tested mounting the sample in the measurement chamber and filling the jars with a specific solvent. The reflectance spectra were collected continuously as a function of time. Due to the gradual evaporation of the solvent, the molecules enter within the PC porosity and determine a change of the effective refractive index and a wavelength shift of the diffraction peak (specifically a red shift since the effective refractive index increases). When all the pore volume is completely saturated, the reflectance peak wavelength reaches a plateau value and the response of the PC can be considered as complete. An example of the maximum reflectance peak redshift registered for ethanol saturated vapour is reported in figure SI_3. The measured redshift of about 50 nm produces also a sensible change in the colour of the PC as shown in figure SI_4. Fig. 4 shows the time dependence of the redshift (difference of the diffraction peak wavelength with and without alcohol) of the PC in the presence of the different pure alcohols and water. The slope of the initial part of the curves is closely related to the vapour tension of the alcohols. A greater vapour pressure corresponds to a higher slope indicating that a more volatile alcohol needs less time to saturate all the space in the chamber and in the pores of the PC. However, if the alcohols remained in the gaseous phase in the pores, the change in the effective refractive index of the PC should be quite small and this could not justify the intense redshifts measured. Such a high variation can rather be ascribed to a condensation of the VOCs between PC particles. The process occurring in the measuring chamber is as follows: the alcohol evaporating from the little containers fills all the empty spaces and also condenses on the PC surface penetrating into its pores as a liquid. We calculated the expected maximum redshift, when the voids between PC particles are completely filled with a specific alcohol, by using equation (2) where the factor f is fixed at 0.72 (estimated filling factor for our PC) and n_m is the refractive index of the selected alcohol as reported in Table 1. The values of the refractive index were extrapolated from different works in literature (reported in the last column of the table) for a temperature of 24 °C and an average humidity of 45%. The calculated $n_{eff.}$ was substituted into equation (1) and the diffraction peak wavelength was calculated with a fixed sphere diameter (D = 250 nm). The obtained values were compared to the experimental data and the results are reported in Fig. 5. The experimental redshifts (yellow bars) are always greater than the calculated ones (red bars), except for water where the behaviour is opposite. To justify our results, a second effect, in addition to the simple change of effective refractive index, has to be taken into account. Our tentative hypothesis is based on a possible swelling of PS particles induced by the alcohols. We estimated the increment of the average sphere diameter necessary to justify the experimentally measured redshifts and ascribed this increment to a swelling of the nanobeads induced by the contact with the alcohol. The percentage increment of the sphere diameter is reported in Table SI_1 of the supporting

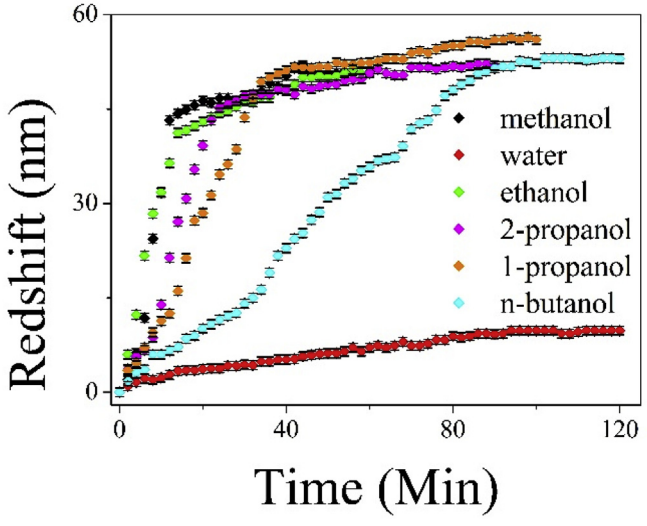

Fig. 4. Time dependence of the redshift of the selected VOCs and water. All the alcohols reach a plateau value in different times depending on their vapour tension, while water presents an anomalous behaviour.

Table 1
Refractive indexes of analyzed solvents at 24 °C and 45% humidity.

Solvent	Refractive index	Ref. Number
Methanol	1.329	[28], [48], [52]
Water	1.334	[53]
Ethanol	1.361	[28], [48], [54]
2-propanol	1.378	[28], [55]
1-propanol	1.386	[28], [56]
n-butanol	1.399	[28], [40], [56]

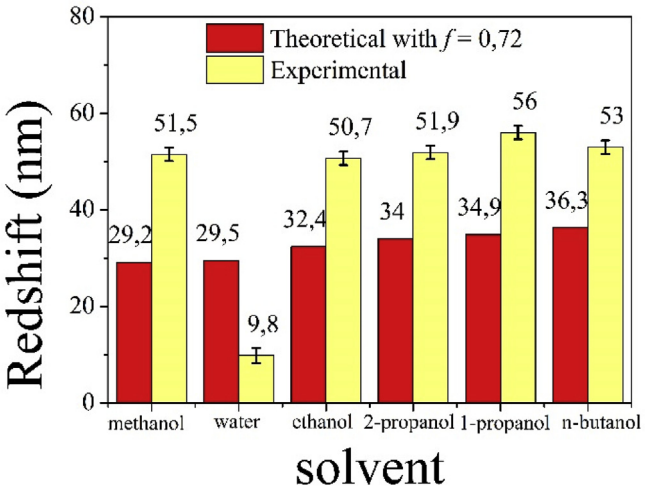

Fig. 5. Comparison between theoretical calculation of the redshift (red bars) and experimental data (yellow bars). (For interpretation of the references to colour in this figure legend, the reader is referred to the Web version of this article.)

information, as diameter swelling, for all the investigated solvents. In order to have an experimental evaluation of the diameter swelling we performed a Dynamic Light Scattering (DLS) characterization. However, the spreading of the average sphere diameters shown in figure SI_5 hampered an unequivocal determination of the swelling itself. We tried to measure the swelling also with a careful determination of the particle diameter by atomic force microscopy in air and liquid but the measurement gave not clear results. On this regard, to have an independent measure of the swelling we performed measurements on polystyrene bulk samples (pellets of about 2 mm in length) immersed for 4 h in the different solvents, comparing the bulk weight after and before the immersion. The results are reported in Table SI_2 as weight swelling in the supporting information. Although the two measurements are not quantitatively comparable, the measured weight swelling induced by immersion in the alcohols suggests that our hypothesis on the increase of the dimension of the nanobeads is indeed valid. On the basis of these results we can conclude that the additional redshift registered for all the alcohols investigated can be tentatively ascribed to a swelling process of the PS spheres.

A different mechanism is valid for water. Water shows a small redshift of 9.8 nm even if its refractive index would produce a theoretical redshift of 29.5 nm. It has to be underlined that the vapour pressure of the water is similar to 1-propanol and higher than n-butanol as reported in Table SI_3 in the supporting information. This indicates that the time window of 120 min (Fig. 4) is wide enough to observe the formation of the saturated vapour of water in the experimental chamber and a full interaction between water and PC is reached as with the other solvents. However, this does not happen since, due to the surface nanostructuring of the PC induced by the nanobeads and the very different surface tension of water in comparison with alcohols, the PC is highly hydrophobic as shown in Fig. 6. Consequently, the condensed water on the surface cannot penetrate inside the porous structure and cannot fill completely the voids of the PC as for the other alcoholic solvents. The small effect on the redshift can be ascribed to a thin surface layer of water or only to a partial filling of the upper pores. This interpretation is strongly supported by measuring the redshift induced by water vapour for different PCs with filling factor varying from 0.68 to 0.74. In these cases, we found that the water penetrates more deeply in the structures having smaller filling factor (wider space between the spheres) and consequently the measured relative redshift was higher. On the basis of these results we may suppose that water wets only the first 8–9 layers of the entire photonic crystal composed by about 25 layers or wets, but only partially, deeper layers giving a reduced effect on the reflectance redshift with respect to what expected for a complete filling of the pores.

An important issue of a sensor is the reversibility, i.e. the possibility to use it several times without damage or reduced response. On this purpose, we checked the reversibility of our polystyrene PC optical sensors. When the sensing measurement was finished and after a waiting time of about 10 min with the chamber opened in order to allow to the solvents to evaporate completely in air, we checked again the reflectivity. Every time after a complete sensing cycle, the measured reflectance spectrum recovered its original shape and intensity, as shown in figure SI_6 for methanol, indicating that our system has a very good reversibility. This property has been checked for all the solvents with similar results.

3.3. Study of different ethanol concentrations

On the basis of the experimental results and the good agreement as regards the vapours of pure VOCs and the hydrophobicity behaviour with water, we decided to try our PCs systems for the measurement of a mixture of two substances, water and ethanol. Specifically, we studied the response of polystyrene PCs to the relative concentration of ethanol in water with the aim of exploiting them as potential breathalyzers. Fig. 7 represents the sensing test at different ethanol concentrations made by changing the relative volumes of water and ethanol. The measured redshift for high concentrations (>70% v_{Ethan}/v_{tot}) is almost constant. The presence of ethanol is so high to saturate completely the voids between PC nanospheres (the pores are totally filled of ethanol). In this case, the response of our system is always maximum and the redshift is about 50 nm, very close to the value of pure ethanol. In the region up to 70% v_{Ethan}/v_{tot}, reported in the figure, the behaviour is characterized by a very good linear dependence of the redshift. In this case the condensation of ethanol is still valid, but its amount is not enough to completely fill the voids of the PCs. The

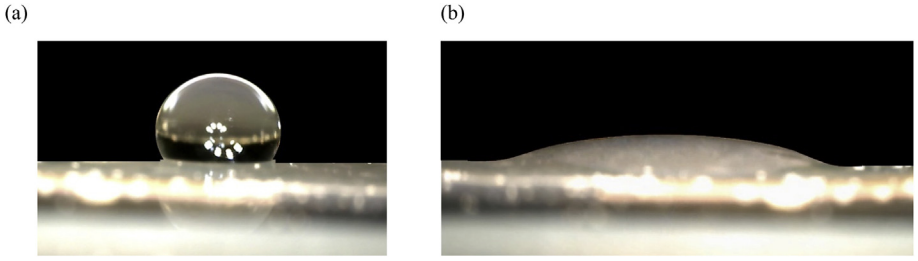

Fig. 6. Hydrophobicity of PC surface: (a) a drop of water shows a small contact area with PC; (b) a drop of ethyl alcohol spreads on a larger area and goes easily inside voids between particles.

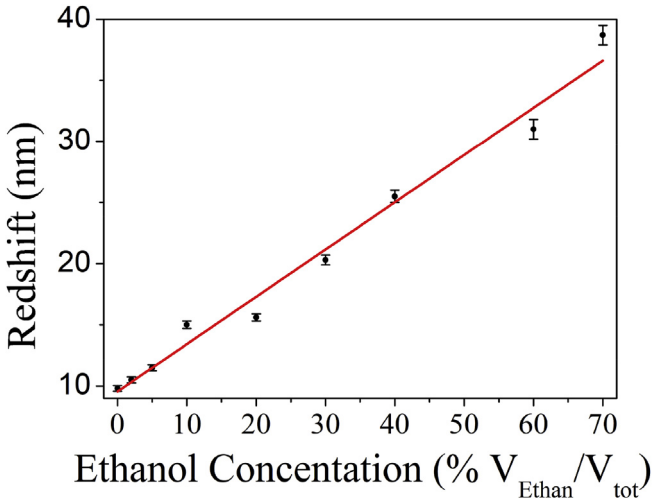

Fig. 7. Redshift of the reflectance band as a function of the ethanol in the range from 0% to 70%.

redshift gradually increases with the increasing concentration of ethanol indicating that the solvent fills the PC pores only partially and proportionally to its concentration. As a reasonable hypothesis we can consider that the $n_{eff.}$ can be written as:

$$n_{eff.} = \sqrt{0.72\, n_p^2 + t\, n_{EtOH.}^2 + g\, n_{water}^2 + (0.28 - t - g) n_{air}^2} \qquad (3)$$

where n_p, n_{EtOH} and n_{air} are the refractive indexes of PC particles, ethanol and air, respectively. The factor t is the volume fraction that ethanol occupies in the spaces between the particles. The factor g is the volume fraction of water inside the PCs voids. Table 2 shows the relative volumes of ethanol and water inserted in the measurement chamber, the percentage of ethanol in liquid phase, the mole fraction of liquid ethanol in the blend, the mole fraction of ethanol in vapour phase and the calculated ethanol vapour concentration in the chamber (in ppm). We calculated the LOD of our system in presence of ethanol considering the value 3σ resulting by the experimental measurement of the reflectance spectrum of the PC in presence of pure water. The LOD was estimated to be 2% ethanol vapour, which corresponds to 1167 ppm. To determine the number of ppm of ethanol vapour presents in the experimental chamber we used the molar fraction of ethanol in alcohol/water solution. Specifically, for the case of 2% the molar fraction of ethanol liquid in the blend water/ethanol was $x_{EtOH}^{Liq} = 0.01$. Using the Antoine's law we estimated the vapour pressure (P^0) of ethanol and water at the temperature of 24 °C and then we calculated, by means of the Raoult's law, the partial pressures of ethanol vapour, water and the air ($P_{tot} = 1$ atm) inside the measuring chamber. From ideal gas law we have determined the mole fraction of ethanol vapour and then the corresponding ppm in the chamber.

In order to compare our results with the results present in literature, we reported in Table 3 a list of PC based sensors for ethanol detection recently developed. This table, even if it is far from to be completely exhaustive, gives a general overview of the research in this field. The value of 1167 ppm is a pretty good value compared to other similar systems but rather high compared to other commercial breathalyzers. However, it has to be considered that a better response is expected with a PC packed more tightly (having filling factor $f = 0.74$) where the contribution of the water to the redshift is considerably less. In addition, the easiness of the synthesis process of polystyrene PCs and the low cost of production make these systems valid candidates to be studied more carefully in the next future.

4. Conclusions

We have developed a photonic crystal based on self-assembled polystyrene nanobeads, which could be used as optical sensor. This device is able to detect the presence of different alcohols (methanol, ethanol, isopropanol, 1-propanol and n-butanol) by a changing in the reflectance spectrum induced by the condensation of the

Table 2
Ethanol concentrations in liquid phase and in vapour phase inside the measuring chamber.

Liquid phase EtOH:H_2O (*vol:vol*)	Percentage of EtOH in liquid phase	EtOH in liquid phase (mole fraction)	EtOH in vapour phase (mole fraction)	EtOH in vapour phase (ppm)
1: 49	2%	0.010	7.26×10^{-4}	1167
1: 19	5%	0.025	1.84×10^{-3}	2962
1: 9	10%	0.052	3.78×10^{-3}	6067
1: 4	20%	0.110	8.02×10^{-3}	12827
1: 2.3	30%	0.175	0.0127	20244
1: 1.5	40%	0.249	0.0181	28678
1.5: 1	60%	0.426	0.0309	48643
2.3: 1	70%	0.536	0.0389	60818
4: 1	80%	0.664	0.0482	74888
9: 1	90%	0.817	0.0593	91342
10: 0	100%	1.000	0.0726	110743

Table 3
PC based sensors for detection of ethanol.

Smallest detectable concentration of ethanol	Ref. Number	State of solution	Type of device
2% (v_{Ethan}/v_{Tot})	This Work	Vapour	PS opal film
0,5% (v_{Ethan}/v_{Tot})	[57]	Liquid	A porphyrin in a polymer matrix as inverse opal film
10% (v_{Ethan}/v_{Tot})	[30]	Liquid	TiO_2 inverse opal film
10% (v_{Ethan}/v_{Tot})	[31]	Liquid	TiO_2 inverse opal film
10% (v_{Ethan}/v_{Tot})	[27]	Vapour	PS opal infiltrated with HEMA/AA/PEG_{200}DMA
10% (v_{Ethan}/v_{Tot})	[58]	Vapour	HEMA/AA/PEG_{200}DMA hydrogel inverse opal
20% (v_{Ethan}/v_{Tot})	[28]	Liquid	PS opal infiltrated with PDMS
50 ppm	[26]	Vapour in nitrogen atmosphere	PMMA opal infiltrated with methylcellulose

vapours inside the pores of the PC. In particular, we detected a substantial wavelength redshift of the reflectance peak, that we ascribed to the increase of the effective refractive index of the system and to the swelling of PS spheres induced by the alcohols. The PCs showed a complete reversibility with all the solvents tested indicating that they can be used several times. Such systems presented a very poor response to the water thanks to the surface nanostructuring of the PC, which prevents the infiltration of water inside the pores. On the basis of these properties, we tested the response of our systems to a mixture of two substances, water and ethanol, with the aim of exploiting them as potential breathalyzers. PS photonic crystals demonstrated to be able to sense different concentration of ethyl alcohol in various water/ethanol solutions, with a LOD of 2% v_{Ethan}/v_{tot}. This limit even if rather high compared to other commercial breathalyzers, is worthwhile for the easiness of the synthesis process and the low cost of production and makes these systems valid candidates to be further investigated.

Acknowledgements

The authors thank prof. Ilaria Cacciotti of the Engineering Department, University of Rome “Niccolò Cusano”, dr. Mauro Bragaglia of the Enterprise Engineering Department of the University of Rome Tor Vergata and prof. Iole Venditti of the Chemistry Department of the University of Rome Sapienza for their precious help in SEM image and DLS characterization. The authors gratefully acknowledge the financial support of the University of Rome Tor Vergata through the Consolidate Foundations program.

Appendix A. Supplementary data

Supplementary data related to this article can be found at https://doi.org/10.1016/j.matchemphys.2018.03.039.

References

[1] J.E. Marcovecchio, S.E. Botté, C.E. Domini, R.H. Freije, Heavy metals, major metals, trace elements, in: L.M.L. Nollet, L.S.P. De Gelder (Eds.), Handbook of Water Analysis, third ed., CRC press, New York (, 2013.
[2] P.L. Kinney, Climate change, air quality, and human health, Am. J. Prev. Med. 35.5 (2008) 459–467.
[3] L. Järup, Hazards of heavy metal contamination, Br. Med. Bull. 68.1 (2003) 167–182.
[4] S. Khan, M. Shahnaz, N. Jehan, S. Rehman, M.T. Shah, I. Din, Drinking water quality and human health risk in Charsadda district, Pakistan, J. Clean. Prod. 60 (2013) 93–101.
[5] P. Prosposito, F. Mochi, E. Ciotta, M. Casalboni, F. De Matteis, I. Venditti, L. Fontana, G. Testa, I. Fratoddi, Hydrophilic silver nanoparticles with tunable optical properties: application for the detection of heavy metals in water, Beilstein J. Nanotechnol. 7 (2016) 1654–1661.
[6] E. Ciotta, S. Paoloni, P. Prosposito, P. Tagliatesta, C. Lorecchio, I. Venditti, R. Pizzoferrato, Sensitivity to heavy-metal ions of unfolded fullerene quantum dots, Sensors 17 (2017) 2614, 11.
[7] B. Brunekreef, S.T. Holgate, Air pollution and health, Lancet 360.9341 (2002) 1233–1242.
[8] J.M. Balbus, A.B.A. Boxall, R.A. Fenske, T.E. McKone, L. Zeise, Implications of global climate change for the assessment and management of human health risks of chemicals in the natural environment, Environ. Toxicol. Chem. 32.1 (2013) 62–78.
[9] I.R. Lake, C.D. Foxall, A.A. Lovett, A. Fernandes, A. Dowding, S. White, M. Rose, Effects of river flooding on PCDD/F and PCB levels in cows' milk, soil, and grass, Environ. Sci. Technol. 39.23 (2005) 9033–9038.
[10] World Health Organisation (WHO), Indoor Air Quality: Organic Pollutants, EURO Reports and Studies No III, World Health Organisation, Copenhagen, Denmark, 1989.
[11] J.J. Shah, H.B. Singh, Distribution of volatile organic chemicals in outdoor and indoor air: a national VOCs data base, Environ. Sci. Technol. 22.12 (1988) 1381–1388.
[12] J.A. Kruse, Methanol poisoning, Intensive Care Med. 18.7 (1992) 391–397.
[13] R.J. Slaughter, R.W. Mason, D.M.G. Beasley, J.A. Vale, L.J. Schep, Isopropanol poisoning, Clin. Toxicol. 52.5 (2014) 470–478.
[14] M. Bunc, T. Pezdir, H. Možina, M. Možina, M. Brvar, Butanol ingestion in an airport hangar, Hum. Exp. Toxicol. 25.4 (2006) 195–197.
[15] S. Capone, A. Forleo, L. Francioso, R. Rella, P. Siciliano, J. Spadavecchia, D.S. Presicce, A.M. Taurino, Solid state gas sensors: state of the art and future activities, J. Optoelectron. Adv. Mater. 5.5 (2003) 1335–1348.
[16] S. Badhulika, M.V. Nosang, A. Mulchandani, Conducting polymer coated single-walled carbon nanotube gas sensors for the detection of volatile organic compounds, Talanta 123 (2014) 109–114.
[17] B. Lakard, S. Carquigny, O. Segut, T. Patois, S. Lakard, Gas sensors based on electrodeposited polymers, Metals 5.3 (2015) 1371–1386.
[18] N. Yamazoe, Toward innovations of gas sensor technology, Sensor. Actuator. B Chem. 108.1 (2005) 2–14.
[19] T. Plecenik, M. Moško, A.A. Haidry, P. Ďurina, M. Truchlý, B. Grančič, M. Mikula, Fast highly-sensitive room-temperature semiconductor gas sensor based on the nanoscale Pt–TiO 2–Pt sandwich, Sensor. Actuator. B Chem. 207 (2015) 351–361.
[20] A. Orsini, P.G. Medaglia, D. Scarpellini, R. Pizzoferrato, C. Falconi, Towards high-performance, low-cost quartz sensors with high-density, well-separated, vertically aligned ZnO nanowires by low-temperature, seed-less, single-step, double-sided growth, Nanotechnology 24.35 (2013), 355503.
[21] D.S. Lee, J.K. Jung, J.W. Lim, J.S. Huh, D.D. Lee, Recognition of volatile organic compounds using SnO_2 sensor array and pattern recognition analysis, Sensor. Actuator. B Chem. 77.1 (2001) 228–236.
[22] J. Tamaki, High sensitivity semiconductor gas sensors, Sens. Lett. 3.2 (2005) 89–98.
[23] R. De Angelis, L. D'Amico, M. Casalboni, F. Hatami, W.T. Masselink, P. Prosposito, Photoluminescence sensitivity to methanol vapours of surface InP quantum dot: effect of dot size and coverage, Sensor. Actuator. B Chem. 189 (2013) 113–117.
[24] C. Elosua, I.R. Matias, C. Bariain, F.J. Arregui, Volatile organic compound optical fiber sensors: a review, Sensors 6.11 (2006) 1440–1465.
[25] M. Consales, A. Crescitelli, M. Penza, P. Aversa, P.D. Veneri, M. Giordano, A. Cusano, SWCNT nano-composite optical sensors for VOC and gas trace detection, Sensor. Actuator. B Chem. 138.1 (2009) 351–361.
[26] R. De Angelis, M. Casalboni, F. Hatami, A. Ugur, W.T. Masselink, P. Prosposito, Vapour sensing properties of InP quantum dot luminescence, Sensor. Actuator. B Chem. 162 (2012) 149.
[27] M.M. Salleh, Y. Muhammad, Enriching the selectivity of metalloporphyrins chemical sensors by means of optical technique, Sensor. Actuator. B Chem. 85.3 (2002) 191–196.
[28] F. Wang, Z. Zhu, M. Xue, F. Xue, Q. Wang, Z. Meng, W. Lu, W. Chen, F. Qi, Z. Yan, Cellulose photonic crystal film sensor for alcohols, Sensor. Actuator. B Chem. 220 (2015) 222–226.
[29] R. Pernice, G. Adamo, S. Stivala, A. Parisi, A.C. Busacca, D. Spigolon, M.A. Sabatino, L. D'Acquisto, C. Dispenza, Opals infiltrated with a stimuli-responsive hydrogel for ethanol vapor sensing, Opt. Mater. Express 3.11 (2013) 1820–1833.
[30] C. Fenzl, T. Hirsch, O.S. Wolfbeis, Photonic crystal based sensor for organic solvents and for solvent-water mixtures, Sensors 12.12 (2012) 16954–16963.
[31] H. Xu, P. Wu, C. Zhu, A. Elbaz, Z.Z. Gu, Photonic crystal for gas sensing, J. Mater. Chem. C 1.38 (2013) 6087–6098.
[32] J. Li, T. Zheng, A comparison of chemical sensors based on the different ordered inverse opal films, Sensor. Actuator. B Chem. 131.1 (2008) 190–195.
[33] W.K. Kuo, H.P. Weng, J.J. Hsu, H.H. Yu, Photonic crystal-based sensors for detecting alcohol concentration, Appl. Sci. 6.3 (2016) 67.
[34] C.Y. Kuo, S.Y. Lu, S. Chen, M. Bernards, S. Jiang, Stop band shift based chemical sensing with three-dimensional opal and inverse opal structures, Sensor. Actuator. B Chem. 124.2 (2007) 452–458.
[35] R. De Angelis, I. Venditti, I. Fratoddi, F. De Matteis, P. Prosposito, I. Cacciotti, L. D'Amico, F. Nanni, A. Yadav, M. Casalboni, M.V. Russo, From Nanosphere to microribbons: self-assembled Eosyn Y doped PMMA nanoparticles as photonic crystals, J. Colloid Interface Sci. 414 (2014) 24–32.
[36] Eli Yablonovitch, Inhibited spontaneous emission in solid-state physics and electronics, Phys. Rev. Lett. 58.20 (1987) 2059.
[37] A. Yadav, R. De Angelis, M. Casalboni, F. De Matteis, P. Prosposito, F. Nanni, I. Caciotti, Spectral properties of self-assembled polystyrene nanospheres photonic crystals doped with luminescent dyes, Opt. Mater. 35 (2013) 1538–1543.
[38] M.S. Reddy, S. Kedia, R. Vijaya, A.K. Ray, S. Sinha, I.D. Rukhlenko, M. Premaratne, Analysis of lasing in dye-doped photonic crystals, IEEE Photon. J. 5 (1) (2013), 4700409.
[39] S. Schutzmann, I. Venditti, P. Prosposito, M. Casalboni, M.V. Russo, High-energy angle resolved reflection spectroscopy on three-dimensional photonic crystals of self-organized polymeric nanospheres, Optic Express 16.2 (2008) 897–907.
[40] Y. Zhang, Q. Fu, J. Ge, Photonic sensing of organic solvents through geometric study of dynamic reflection spectrum, Nat. Commun. 6 (2015) 7510.
[41] J.D. Joannopoulos, S.G. Johnson, J.N. Winn, R.D. Meade, Photonic Crystals Molding the Flow of Light, Princeton University Press, New Jersey (, 2008.
[42] M.J. Serpe, Y. Kang, Q.M. Zhang, Photonic Materials for Sensing, Biosensing and Display Devices, Springer series in materials science, 2016.
[43] C.G. Schäfer, M. Gallei, G.P. Hellmann, M. Biesalski, M. Rehahn, Multi-stimuli-responsive Elastomeric Opal Films: Processing, Optics and Applications, vol. 8816, SPIE NanoScience Engineering International Society for Optics and Photonics, 2013, 88160V.
[44] B.T. Borille, T.R. Fiorentin, B.C. Coppe, E. Comiran, A.L.B. Jacques, T.R.V. Sousa, G.G. Pasa, F. Pechansky, S.M. de Jezus Castro, R.P. Limberger, Detection of ethanol in Brazilian gasoline station attendants, Anal. Meth. 7.7 (2015)

2936–2942.
[45] United Nation Road Safety, Drinking and Driving – an International Good Practice Manual, 2017. http://www.who.int/roadsafety/projects/manuals/alcohol/en/. (Accessed 21 June 2017).
[46] E. Bihar, Y. Deng, T. Miyake, M. Saadaoui, G.G. Malliaras, M. Rolandi, A disposable paper breathalyzer with an alcohol sensing organic electrochemical transistor, Sci. Rep. 6 (2016), 27582.
[47] P. Prosposito, M. Casalboni, E. Orsini, C. Palazzesi, F. Stella, UV-nanoimprinting lithography of Bragg Gratings on hybrid sol-gel based channel waveguides, Solid State Sci. 12 (11) (2010) 1886–1889.
[48] W.K. Kuo, H.P. Weng, J.J. Hsu, H.H. Yu, A bioinspired color-changing polystyrene microarray as a rapid qualitative sensor for methanol and ethanol, Mater. Chem. Phys. 173 (2016) 285–290.
[49] C. Fenzl, T. Hirsch, O.S. Wolfbeis, Photonic crystals for chemical sensing and biosensing, Angew. Chem. Int. Ed. 53.13 (2014) 3318–3335.
[50] G. Pan, B. Zu, X. Guo, Y. Zhang, C. Li, H. Zhang, Preparation of molecularly imprinted polymer microspheres via reversible addition–fragmentation chain transfer precipitation polymerization, Polymer 50.13 (2009) 2819–2825.
[51] A. Nematollahzadeh, M.J. Abdekhodaie, A. Shojaei, Submicron nanoporous polyacrylamide beads with tunable size for verapamil imprinting, J. Appl. Polym. Sci. 125.1 (2012) 189–199.
[52] H. El-Kashef, The necessary requirements imposed on polar dielectric laser dye solvents, Phys. B Condens. Matter 279 (2000) 295–301.
[53] M. Daimon, A. Masumura, Measurement of the refractive index of distilled water from the near-infrared region to the ultraviolet region, Appl. Optic. 46.18 (2007) 3811–3820.
[54] J. Rheims, J. Köser, T. Wriedt, Refractive-index measurements in the near-IR using an Abbe refractometer, Meas. Sci. Technol. 8 (1997) 601–605.
[55] I.Z. Kozma, P. Krok, E. Riedle, Direct measurement of the group-velocity mismatch and derivation of the refractive-index dispersion for a variety of solvents in the ultraviolet, J. Opt. Soc. Am. B 22 (2005) 1479–1485.
[56] K. Moutzouris, M. Papamichael, S.C. Betsis, I. Stavrakas, G. Hloupis, D. Triantis, Refractive, dispersive and thermo-optic properties of twelve organic solvents in the visible and near-infrared, Appl. Phys. B 116 (2013) 617–622.
[57] A.K. Yetisen, M.M. Qasim, S. Nosheen, T.D. Wilkinson, C.R. Lowe, Pulsed laser writing of holographic nanosensors, J. Mater. Chem. C 2.18 (2014) 3569–3576.
[58] C. Dispenza, M.A. Sabatino, S. Alessi, G. Spadaro, L. D'Acquisto, R. Pernice, G. Adamo, S. Stivala, A. Parisi, P. Livreri, A.C. Busacca, Hydrogel films engineered in a mesoscopically ordered structure and responsive to ethanol vapors, React. Funct. Polym. 79 (2014) 68–76.